Intensity of parametric fluorescence pumped by ultrashort pulses

Jan Chwedeńczuk
Institute of Theoretical Physics, Warsaw University, Hoża 69, 00-681 Warsaw, Poland

Wojciech Wasilewski
Institute of Experimental Physics, Warsaw University, Hoża 69, 00-681 Warsaw, Poland

(Received 21 April 2008; published 15 December 2008)

We investigate intensity of the parametric down conversion of ultrashort, ultraviolet pulse both in a low- and high-conversion regime. In the first regime, we develop a simple analytical expressions for the photon flux of the fluorescence. Numerical simulations using three-dimensional stochastic Wigner method provide results in the latter regime. We find that the perturbative approximation for the photon flux as a function of the wavelength of the signal and the observation angle, quantitatively describes even the nonperturbative regime. For short pump pulses the intensity of the fluorescence is highest at frequencies where the group velocities of the pump and the down-conversion are equal. For longer pump pulses this requirement is gradually relaxed. Additionally, for small pump beams, the intensity strongly depends on the spatial divergence between interacting fields.

DOI: 10.1103/PhysRevA.78.063823 PACS number(s): 42.65.Lm, 42.65.Yj, 42.65.Re

I. INTRODUCTION

Quantum parametric fluorescence is one of the most frequently used sources of nonclassical radiation. In the low gain regime, the parametric process is used as a robust source of single photons and photon pairs. The parametric fluorescence-based sources allowed for a number of fundamental experiments. Examples include Bell inequality breaking [1], quantum cryptography [2], and quantum teleportation [3]. Nowadays the effort focuses on engineering the correlation properties [4–7] of such sources. On the other hand, in some experiments intense pump pulses are used, which results in high parametric gain. This regime is characterized by an appreciable amount of multiple pair creation events and most conveniently described by recalling the notion of squeezing [8]. Single or two-mode squeezing described in textbooks can be used to describe realistic multimode parametric amplifier [9] and it turns out that a laboratory device produces a superposition of squeezed states in modes defined both by the nonlinear medium and the pump pulse. High-gain parametric amplifiers are nowadays also frequently used for amplification of ultrashort pulses [10]. In this application the parametric fluorescence is an important and troublesome source of noise.

In this paper we provide a number of original results. We calculate the average angular and spectral intensity of a spontaneous parametric fluorescence. Since parametric fluorescence has quantum origin, its intensity cannot be calculated using classical nonlinear optics. Below, we adopt both a perturbative and stochastic approach for this task. With a few approximations we provide a simple formula for the intensity of the fluorescence in single-pair generation regime. Numerical simulations show, that it qualitatively reproduces main features of the donwn-conversion spectrum in the high gain regime as well.

Our results could be used as guidelines for constructing brighter photon-pair sources. Other application would be optimization of high-gain parametric amplifiers for a minimal contribution of parametric fluorescence [11].

Let us mention that a process analogous to parametric down-conversion is observed in physics of cold atoms. When a pair of Bose-Einstein condensates collide, a halo of spontaneously scattered of atoms is observed [12,13]. Stochastic methods used for description of this process proved extremely successful [14,15] and we adopted them to obtain results presented below.

The paper is organized as follows. In Sec. II we recall some basics of the theory of the parametric down-conversion. In Sec. III, we calculate the photon flux in the perturbative regime. In Sec. IV, we compare these results with numerical predictions in the high-gain regime. We conclude in Sec. V.

II. THEORY OF THE PARAMETRIC DOWN-CONVERSION

A process of parametric down-conversion takes place in a crystal with nonzero second order nonlinear susceptibility tensor $\chi^{(2)}$ when it is irradiated with a pump beam. Upon passing through the nonlinear medium each of the pump pulses gives rise to photon pairs which form the parametric fluorescence. Below, we formulate a theoretical model describing the nonlinear interaction which allows for calculation of the fluorescence intensity.

We assume that the medium interfaces are parallel to the x-y plane, while fields propagate along the z coordinate, as depicted in Fig. 1. We expand all the fields involved in the interaction using an approach from nonlinear optics. At each z an expansion in a basis of plane waves with frequency ω and wave vector k_x, k_y is given, while z parametrizes the development of the evolution. To shorten the notation, let us denote the triple (ω,k_x,k_y) parametrizing each plane-wave component of the fields by κ. For concreteness, we consider type-I interaction in β-barium borate (BBO) in which pump propagates as an e ray while the fluorescence as an o ray. Results can, however, be easily generalized for any nonlinear crystal by substituting its particular dispersion relation in the

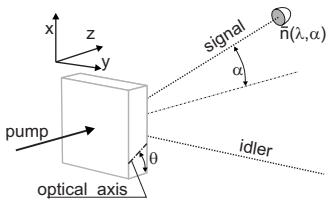

FIG. 1. Scheme of a measurement of the photon flux $\bar{n}(\lambda,\alpha)$ of the spontaneous parametric fluorescence. The nonlinear crystal is pumped along the z axis. Out of the emerging parametric fluorescence we observe a small portion at the wavelength λ propagating at an angle α to the z axis in the x-z plane.

formulas below. This will, in general, break a cylindrical symmetry found in type-I phase matching, but the essential results remain unchanged.

Let us consider a regime in which the pump consists of intense pulses described by a classical envelope $\tilde{A}_p(\kappa_p,z)$ in the frequency domain, spanned by $\kappa_p=(\omega_p,k_{px},k_{py})$. The evolution of the pump pulse $\tilde{A}_p(\kappa_p,z)$ along z is determined by the dispersion relation of the crystal. A nonlinear interaction with the fluorescence field can be neglected, since the intensity of the pumping field is large and its depletion due to parametric down-conversion is minimal. This condition is readily satisfied in many experiments. Note that the intensity of the pump is also assumed large enough to neglect any quantum fluctuations and describe it by a classical field.

For a pump propagating as an e-ray in a crystal cut at an angle θ to the z axis the dispersion relation of the crystal reads

$$\frac{\omega_p^2}{c^2}=\frac{(k_{px}\cos\theta-k_{pz}\sin\theta)^2}{n_e^2(\omega_p)}+\frac{(k_{pz}\cos\theta+k_{px}\sin\theta)^2+k_{py}^2}{n_o^2(\omega_p)}, \tag{1}$$

where $n_o(\omega_p)$ and $n_e(\omega_p)$ are ordinary and extraordinary refractive indices of the crystal. For each plane wave component of pump field with given $\kappa_p=(\omega_p,k_{px},k_{py})$ the above relation fixes the z component of the wave vector k_{pz} at a value $k_{pz}(\kappa_p)$. During propagation along z each of the plane-wave components will acquire phase equal to $\exp[ik_{pz}(\kappa_p)L]$. Thus, the equation of evolution of the pump pulse $\tilde{A}_p(\kappa_p,z)$ can be written as [16]

$$\frac{\partial}{\partial z}\tilde{A}_p(\kappa_p,z)=ik_{z,p}(\kappa_p)\tilde{A}_p(\kappa_p,z). \tag{2}$$

On the contrary, the parametric fluorescence has to be described by a quantum field. We expand this field in a basis of plane waves parametrized by $\kappa=(\omega,k_x,k_y)$, which corresponds to the following expression for the field operator $\hat{E}(x,y,z,t)$ in the position space [17]:

$$\hat{E}(x,y,z,t)=i\int\frac{d^3\kappa}{(2\pi)^3}\sqrt{\frac{\hbar\omega}{2\epsilon_0\sqrt{n(\omega)}}}\hat{a}(\kappa,z)e^{ik_xx+ik_yy-i\omega t}+\text{H.c.} \tag{3}$$

Here $\hat{a}(\kappa,z)$ form a complete set of bosonic annihilation operators at each z while $n(\omega)$ is the index of refraction of the medium. The evolution of the parametric fluorescence is also largely determined by the crystal dispersion, which determines k_z for each plane wave component with given $\kappa=(\omega,k_x,k_y)$ at a value $k_z=k_z(\kappa)$,

$$k_z(\kappa)=\sqrt{n_o^2\frac{\omega^2}{c^2}-k_x^2-k_y^2}. \tag{4}$$

Additionally, the signal field interacts with the pump pulse via the second order nonlinearity. Classical equations, describing propagation of the fluorescence field through the crystal are well known [18]. Quantization of the signal field corresponds to replacement of c-number amplitudes and their complex conjugates of plane-wave modes by annihilation and creation operators $\hat{a}(\kappa,z)$ and $\hat{a}^\dagger(\kappa,z)$ and leads to the Heisenberg equations for their evolution:

$$\frac{\partial}{\partial z}\hat{a}(\kappa,z)=ik_z(\kappa)\hat{a}(\kappa,z)+\frac{1}{L_{\text{NL}}}\int d\kappa'\frac{\tilde{A}_p(\kappa',z)}{A_0}\hat{a}^\dagger(\kappa'-\kappa,z). \tag{5}$$

Here, A_0 is the maximal amplitude of the pump pulse in time-position space $A_0=\int d^3\kappa_p\tilde{A}_p(\kappa_p)$, while L_{NL} is a nonlinear length, a constant which determines a characteristic length over which nonlinear interaction produces a few photon pairs, defined as

$$\frac{1}{L_{\text{NL}}}=\frac{\omega_p^2d_{\text{eff}}A_0}{8c^2k(\omega_p/2)}. \tag{6}$$

For a crystal of a length L and given pump pulses $\tilde{A}_p(\kappa,z=0)$ at the crystal entrance we can find Green functions $C(\kappa,\kappa')$ and $S(\kappa,\kappa')$ of Eq. (5) and express the fluorescence field at the crystal exit face $\hat{a}_{\text{out}}(\kappa)=\hat{a}(\kappa,L)$ in terms of that on the input face $\hat{a}_{\text{in}}(\kappa)=\hat{a}(\kappa,0)$:

$$\hat{a}_{\text{out}}(\kappa)=\int d\kappa'[C(\kappa,\kappa')\hat{a}_{\text{in}}(\kappa')+S(\kappa,\kappa')\hat{a}_{\text{in}}^\dagger(\kappa')]. \tag{7}$$

The above equation gives a complete quantum description of the parametric amplifier. In our case it is highly redundant, since we are interested in the average intensity of the parametric fluorescence $\langle\hat{a}^\dagger(\kappa)\hat{a}(\kappa)\rangle=\langle\hat{n}(\kappa)\rangle$ as a function of the frequency and direction, both contained in κ. In the following section, we use Eq. (7) only as a backbone for developing more specialized results.

III. PERTURBATIVE APPROXIMATION

In this section we discuss the properties of the average intensity of the parametric fluorescence calculated in the first order approximation with respect to the strength of the nonlinearity $1/L_{\text{NL}}$. This approximation physically corresponds to a situation when the fluorescence field consists of a single or a few pairs of photons emitted into distinct frequency or angular regions. It is expected that as soon as the pump becomes so intense that the photons are emitted in bunches, perturbative expansion fails. However, as we show, some results inferred from the perturbative approach, can be directly applied even in the high-gain regime.

Our starting point will be an expression directly related to the well known biphoton wave function which have been introduced in works on spontaneous parametric down-conversion in the context of photon sources [4]. However, the intensity of such sources have, surprisingly, received very little theoretical attention. In this section we apply formalism developed in previous work [9] to calculate the intensity of the parametric fluorescence. This new result can be expressed in a simple form after a few justified approximations.

In order to calculate $\bar{n}(\kappa)=\langle\hat{a}^{\dagger}(\kappa)\hat{a}(\kappa)\rangle$ which describes the intensity of the parametric fluorescence, we first obtain an approximate Green functions $C(\kappa,\kappa')$ and $S(\kappa,\kappa)$. This is done by transforming into the interaction picture, which is accomplished by substituting

$$\hat{a}(\kappa,z)=\exp[ik_z(\kappa)z]\hat{a}_I(\kappa,z) \tag{8}$$

into Eq. (5). The resulting equation of evolution of $\hat{a}_I(\kappa,z)$ contains only nonlinear term and can be easily solved perturbatively with respect to $1/L_{\mathrm{NL}}$ [9]. The first order solution is next compared with a general form given by Eq. (7). The $C(\kappa,\kappa')$ function in the lowest order describes simple dispersive evolution of the fluorescence field passing through the crystal

$$C(\kappa,\kappa')=\delta(\kappa-\kappa')e^{ik_z(\kappa)L}, \tag{9}$$

while the $S(\kappa,\kappa')$ describes the process of pair generation

$$S(\kappa,\kappa')=\frac{L\tilde{A}_p(\kappa+\kappa')}{L_{\mathrm{NL}}A_0}e^{i[k_z(\kappa)-k_z(\kappa')](L/2)}\mathrm{sinc}\left(\frac{L\Delta k(\kappa,\kappa')}{2}\right), \tag{10}$$

where $\Delta k(\kappa,\kappa')$ is a wave vector mismatch between plane-wave components of the fluorescence characterized by spatiotemporal frequencies κ and κ' and coupled plane wave component of the pump characterized by spatiotemporal frequency $\kappa+\kappa'$:

$$\Delta k(\kappa,\kappa')=k_{pz}(\kappa+\kappa')-k_z(\kappa)-k_z(\kappa'). \tag{11}$$

Let us note that $S(\kappa,\kappa')$ is directly realted to the biphoton wave function and differs from it just by phase factor [9].

The above result can be used to calculate the intensity of spontaneous parametric fluorescence emitted at a certain direction in a certain frequency, corresponding to a vector κ:

$$\bar{n}(\kappa)=\langle\hat{a}^{\dagger}_{\mathrm{out}}(\kappa)\hat{a}_{\mathrm{out}}(\kappa)\rangle=\int d^3\kappa'|S(\kappa,\kappa')|^2$$
$$=\left(\frac{L}{L_{\mathrm{NL}}}\right)^2\int d^3\kappa'\left|\frac{\tilde{A}_p(\kappa+\kappa')}{A_0}\right|^2\mathrm{sinc}^2\left(\frac{L\Delta k(\kappa,\kappa')}{2}\right). \tag{12}$$

The above integral can be given a meaningful physical interpretation. Observation of a signal photon testifies generation of the idler photon. In our case the first is detected using narrow-band filters and is nearly plane-wave and monochromatic, characterized by vector κ. Thus, all the frequency and direction distribution present in the pump is transferred to the idler photon, as depicted in Fig. 2. Each plane-wave component of the idler characterized by κ' can support the production of signal characterized by κ if the pair in question is phase matched with a pump component characterized by $\kappa+\kappa'$, i.e., the phase mismatch $L\Delta k(\kappa,\kappa')$ is small.

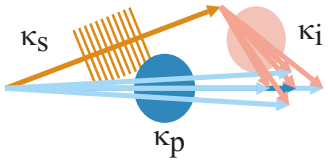

FIG. 2. (Color online) Observation of a plane-wave monochromatic component of the fluorescence field, described by wave vector κ_s, leads to projection of the conjugate idler field into a pulsed form, described by wave vectors κ_i. The idler wave packet takes up all the frequency and wave vector span of the pump pulse, described by wave vectors κ_p.

The integral given in Eq. (12) cannot be evaluated analytically in case of pulsed pumping, when $\tilde{A}_p(\kappa_p,z)$ is nonzero over a finite range of κ. However, the integrand can be approximated with a Gaussian function. First, let us assume a Gaussian form of the pump amplitude at the crystal entrance face $\tilde{A}_p(\kappa_p,z=0)$, corresponding to a pulse of duration τ_p propagating in a beam of width w_p, centered around frequency $2\omega_0$:

$$\tilde{A}_p(\kappa_p,z=0)=A_0\frac{w_p^2\tau_p}{(2\pi)^{3/2}}\times\exp\left(-\frac{\tau_p^2(\omega-2\omega_0)^2}{2}-\frac{w_p^2(k_x^2+k_y^2)}{2}\right). \tag{13}$$

Concentration of the pump energy around given κ_p together with requirement of phase matching $\Delta k(\kappa,\kappa')<1/L$ reduces the range of spatiotemporal frequencies κ and κ' over which a significant amount of parametric fluorescence is generated. To analyze this effect, let us consider perfectly phase-matched parametric down-conversion of the central plane-wave component of the pump with $\kappa_p=(2\omega_0,0,0)$. This part of the fluorescence consists of a plane wave component pairs characterized by κ and κ' which satisfy the following set of equations:

$$\begin{cases}\kappa+\kappa'=(2\omega_0,0,0),\\ \Delta k(\kappa,\kappa')=0.\end{cases} \tag{14}$$

The first equation corresponds to a requirement that both components of the down-conversion couple to the central component of the pump, while the second equation is the perfect phase matching condition. This is in fact a set of four equations for six components of κ and κ' which defines a two-dimensional surface. Assuming $\kappa=(\omega,k_x,k_y)$ as before, from the first equation we get $\kappa'=(2\omega_0-\omega,-k_x,-k_y)$. Then the solution of the second equation can be cast into the following form:

$$\sqrt{k_x^2+k_y^2}=k^0(\omega). \tag{15}$$

In Appendix A we express $k^0(\omega)$ in terms of material and pump parameters. Equation (15) is an axially symmetric sur-

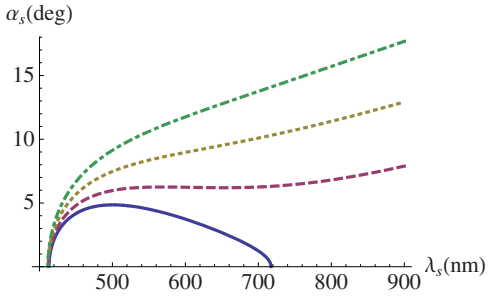

FIG. 3. (Color online) Angle $\alpha_s=\arcsin[ck^0(\omega)/\omega]$ at which perfectly phase-matched fluorescence at the wavelength $\lambda=2\pi c/\omega$ emerges outside the crystal. Plot corresponds to type-I phase matching in BBO pumped at $2\pi c/(2\omega_0)=400$ nm for crystals cut at angles $\theta=29°$ (solid line), 31.3° (dashed line), 35° (dotted line), and 40° (dash-dot line).

face in three-dimensional space of $\kappa=(\omega,k_x,k_y)$, describing plane-wave components of the parametric fluorescence which can be produced from the central component of the pump in a perfectly phase-matched process. In Fig. 3 we plot a section through this surface in the $k_x-\omega$ plane, for parametric down conversion in a BBO crystal pumped at $2\pi c/(2\omega_0)=400$ nm and four different cut angles θ.

As the spatiotemporal frequency of the fluorescence κ deviates from the perfect phase matching surface $k^0(\omega)$ its intensity diminishes. In the region of κ in which the fluorescence intensity is large, the sinc function can be approximated by a Gaussian [19]. Such an approximation fails only for very thick crystals, in which intricacies of the phase matching may play an important role, but the fluorescence emitted in such cases contains very complicated correlations, which render it useless in most of the known applications.

The next step towards Gaussian approximation of the integrand in Eq. (12) is a linearization of the phase mismatch $\Delta k(\kappa,\kappa')$ given by Eq. (11) around points on perfect phase-matching surface. Since it is axially symmetric, we choose points in $k_x>0$ and ω half-plane. For each fixed observation frequency $\omega_{\rm obs}$ we expand phase mismatch $\Delta k(\kappa,\kappa')$ around $\kappa_0=(\omega_{\rm obs},k^0(\omega_{\rm obs}),0)$ and $\kappa_0'=(2\omega_0-\omega_{\rm obs},-k^0(\omega_{\rm obs}),0)$ up to linear terms. This gives (see Appendix B for details)

$$\Delta k_z^{\rm lin}(\kappa,\kappa')=[\omega'-(2\omega_0-\omega_{\rm obs})]\Delta\beta_1'+[k_x-k^0(\omega_{\rm obs})]\Delta\rho_x+k_y\Delta\rho_y+[k_x'+k^0(\omega_{\rm obs})]\Delta\rho_x'+k_y'\Delta\rho_y', \quad (16)$$

where the expansion coefficients equal

$$\Delta\beta_1'=\left.\frac{\partial k_{pz}(\kappa_p)}{\partial\omega'}\right|_{\kappa_p=\kappa_0+\kappa_0'}-\left.\frac{\partial k_z(\kappa')}{\partial\omega'}\right|_{\kappa'=\kappa_0'},$$

$$\Delta\rho_i=\left.\frac{\partial k_{pz}(\kappa_p)}{\partial k_{pi}}\right|_{\kappa_p=\kappa_0+\kappa_0'}-\left.\frac{\partial k_z(\kappa)}{\partial k_i}\right|_{\kappa=\kappa_0},$$

$$\Delta\rho_i'=\left.\frac{\partial k_{pz}(\kappa_p)}{\partial k_{pi}}\right|_{\kappa_p=\kappa_0+\kappa_0'}-\left.\frac{\partial k_z(\kappa')}{\partial k_i'}\right|_{\kappa'=\kappa_0'},$$

$$i=x,y. \quad (17)$$

The above coefficients have simple physical meaning. $\Delta\beta_1'$ is a difference of inverse group velocities between the pump pulse and the fluorescence component characterized by κ', while $\Delta\rho$ give the amount of spatial displacement per unit length between pump pulses and the fluorescence component characterized by κ or κ' in x or y direction. Note, that all the above coefficients depend on the choice of the observation frequency $\omega_{\rm obs}$.

Finally, in Eq. (12) we approximate the sinc function by a Gaussian

$$\mathrm{sinc}^2\left(\frac{L\Delta k_z}{2}\right)\simeq\exp\left(-\frac{L^2}{12}(\Delta k_z^{\rm lin})^2\right) \quad (18)$$

and obtain the following expression for the fluorescence intensity:

$$\bar{n}(\kappa)=\left(\frac{L}{L_{\rm NL}}\right)^2\int d^3\kappa' e^{-(L^2/12)[\Delta k_z^{\rm lin}(\kappa,\kappa')]^2}\left|\frac{\tilde{A}_p(\kappa+\kappa')}{A_0}\right|^2. \quad (19)$$

This integral can be evaluated analytically. Let us substitute $\kappa=\kappa_0=(\omega_{\rm obs},k^0(\omega_{\rm obs}),0)$ which describes the perfect phase-matching line. Then we obtain an estimate of the intensity of the fluorescence emitted at a frequency $\omega_{\rm obs}$ at an angle $\alpha=\arcsin[ck^0(\omega_{\rm obs})/\omega_{\rm obs}]$ to the z axis in the z-x plane

$$n(\omega_{\rm obs},k^0(\omega_{\rm obs}),0)=\frac{w_p^2\tau_p}{4\pi^{3/2}}\left(\frac{L}{L_{\rm NL}}\right)^2\times\left[4+\frac{L^2(\Delta\rho_x'^2+\Delta\rho_y'^2)}{w_p^2}+\left(\frac{L\Delta\beta_1'}{\tau_p}\right)^2\right]^{-1/2}. \quad (20)$$

Let us consider the dependence of the intensity of the fluorescence along the perfect phase-matching line $n(\omega_{\rm obs},k^0(\omega_{\rm obs}),0)$ on the frequency $\omega_{\rm obs}$ at which we observe it. Note again, that observation of the fluorescence signal at the frequency $\omega_{\rm obs}$ testifies generation of the conjugate (idler) photons at the frequency $2\omega_0-\omega_{\rm obs}$. It turns out, that the propagation properties of the idler photons influence the intensity of the signal. In particular three parameters, which vary with $\omega_{\rm obs}$ come into play. The first is the ratio of the temporal walk-off between pump pulse and conjugate photons over the crystal length $L\Delta\beta_1'$ to the pump pulse duration τ_p. The other two measure the ratio of the transverse displacement between the pump pulse and conjugate photons $L\Delta\rho_x'$ and $L\Delta\rho_y'$ to the pump pulse width w_p.

This can be understood by reconsidering the picture drawn in Fig. 2. As we argued before, observation of a nearly plane-wave signal transfers the frequency and wave vector distribution of the pump to the idler photon, which takes a form of a short pulse and propagates according to the crystal dispersion. Usually, it quickly diverges from the pump pulse—the expression in the square brackets in Eq. (20) is large. However, for some frequencies of the signal $\omega_{\rm obs}$ the idler propagates with the pump for a longer distance which

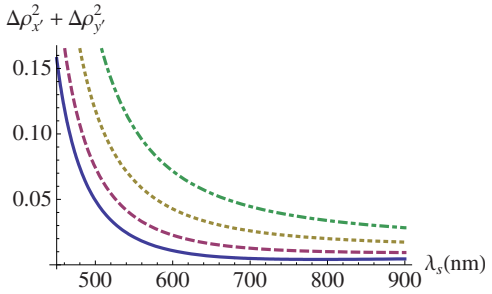

FIG. 4. (Color online) Square idler spatial displacement coefficient $\Delta\rho_{x'}^2+\Delta\rho_{y'}^2$ in BBO for four different crystal cut angles $\theta=29°$ (solid line), $\theta=31.3°$ (dashed line), $\theta=35°$ (dotted line), and $\theta=40°$ (dot-dashed line).

increases the nonlinear interaction and the photon flux $\bar{n}(\omega_{\rm obs},k^0(\omega_{\rm obs}),0)$.

We plot relevant material coefficients in BBO in the case when it is pumped at 400 nm and cut at four characteristic crystal cut angles θ in Fig. 4 and 5. We also plot the intensity of the fluorescence along the perfect phase-matching line $\bar{n}(\omega_{\rm obs},k^0(\omega_{\rm obs}),0)$ given in Eq. (20) as a function of the wavelength of observation $2\pi c/\omega_{\rm obs}$ in Fig. 6 for a few typical pump pulse durations and widths.

It is worthwhile to consider the features displayed by these plots. For short pump pulses, when temporal walk-off between pump and conjugate photons is more pronounced, the fluorescence intensity reaches local maximum values at a wavelength where this walk-off vanishes, $\Delta\beta_1=0$. For longer pulses the temporal walk-off loses its importance, and the intensity of the fluorescence increases with wavelength due to reduced spatial displacement between the pump and conjugate photons, i.e., $\Delta\rho_x'^2+\Delta\rho_y'^2$.

IV. THREE-DIMENSIONAL STOCHASTIC MODEL

In the previous section we calculated the intensity of the parametric fluorescence in the single pair generation limit. Now we switch to intense-pumping regime, when photons are generated in bunches and perturbative approximation breaks down. Estimation of the fluorescence intensity is of a great importance in novel practical applications of parametric amplifiers. For example, when using this kind of nonlinear interaction to amplify broadband chirped pulses, the parametric fluorescence is a source of large and difficult to avoid noise [11].

In this section we describe a numerical method of solving the dynamics of a coupled pump-signal system given by Eqs. (2) and (5) and estimating the intensity of the parametric fluorescence. We use so-called stochastic Wigner method, which can, in principle, provide exact solutions for linear quantum systems, such as described by Eq. (5). If the Wigner function of the field at the entrance is Gaussian, in particular representing vacuum state, the Wigner function of the final state of the parametric fluorescence will be Gaussian too. It is easily deduced from a general form of the input-output relations given by Eq. (7).

A crucial observation is that if the Heisenberg equation is linear, the evolution of the Wigner function is the same as a classical Liouville equation for the density probability of finding the system in a state with particular electric field. Thus the Wigner function $W[\alpha(\kappa,z)]$ can be interpreted as a probability density of finding the system with a fluorescence field described by a spectral amplitude $\alpha(\kappa,z)$.

Therefore, to find the Wigner function of the fluorescence at the crystal exit face we repeat the following procedure. First we draw an input spectral amplitude $\alpha(\kappa,z=0)$ with

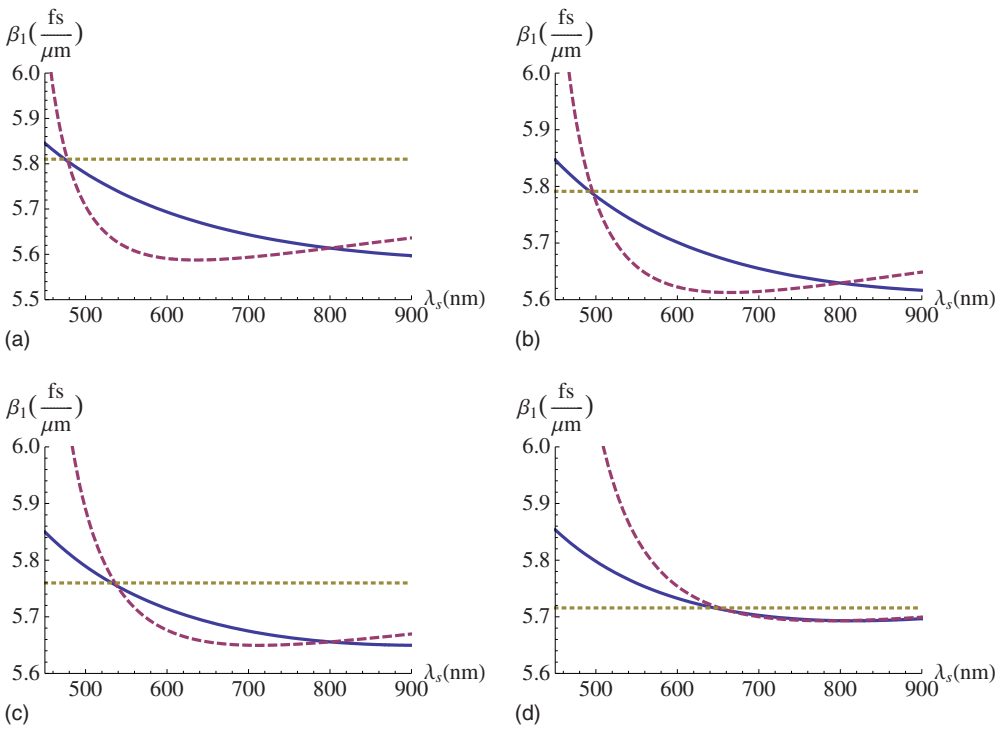

FIG. 5. (Color online) Inverse of the group velocities of pump (dotted line), signal (solid line), and idler (dashed line) for following angles of the crystal setting: (a) $\theta=29°$, (b) $\theta=31.3°$, (c) 35°, and (d) 40°.

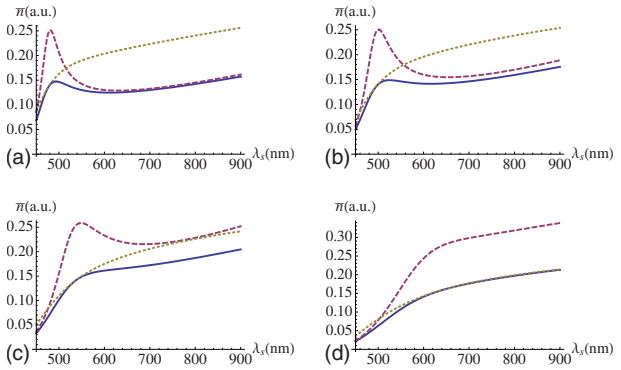

FIG. 6. (Color online) Photon flux of the fluorescence $\bar{n}(\omega_{\mathrm{obs}},k^0(\omega_{\mathrm{obs}}),0)$ along the perfect phase matching line plotted in Fig. 3 calculated using Gaussian approximation for 2-mm-long BBO crystal. Plots are made for four different crystal cut angles (a) $\theta=29°$, (b) 31.3°, (c) 35°, and (d) 40°. Various lines indicate different pump pulse parameters: solid lines correspond to $\tau_p=60$ fs, $w_p=80$ μm, dashed lines correspond to larger pump beam, $\tau_p=60$ fs, $w_p=160$ μm and dotted lines correspond to longer pump pulses $\tau_p=120$ fs, $w_p=80$ μm.

probability given by the vacuum Wigner function

$$W[\alpha(\kappa,z=0)]=\left(\frac{2}{\pi}\right)^N \exp\left(-2\sum_{\kappa}|\alpha(\kappa)|^2\right), \tag{21}$$

where we assumed a finite number N of discrete modes indexed by κ. Next we solve classical equations of propagation of the signal field:

$$\frac{\partial}{\partial z}\alpha(\kappa,z)=ik_z(\kappa)\alpha(\kappa,z)+\int d\kappa' \frac{\tilde{A}_p(\kappa,z)\alpha^*(\kappa-\kappa',z)}{L_{\mathrm{NL}}A_0}. \tag{22}$$

This way we obtain a possible output spectral amplitude $\alpha(\kappa,z=L)$. By repeating this procedure many times, we obtain a set of probable output field amplitudes $\{\alpha(\kappa,z=L)\}$, which approximates Wigner function $W[\alpha(\kappa,z=L)]$. This is schematically illustrated in Fig. 7.

This can be used to calculate the mean photon flux at a given direction and frequency. It equals a mean $|\alpha(\kappa)|^2$ averaged with the Wigner function $W[\alpha(\kappa,z=L)]$ minus

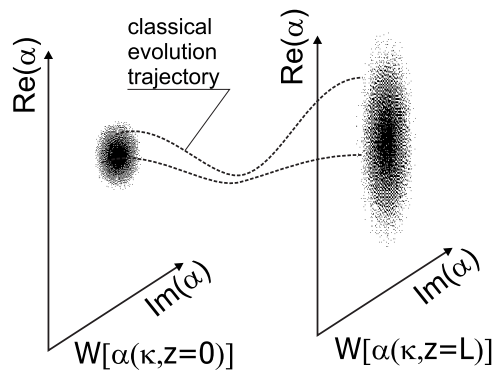

FIG. 7. Graphical illustration of the Wigner method.

vacuum average. Using the set of output amplitudes $\{\alpha(\kappa,z=L)\}$ this is calculated as

$$\bar{n}(\kappa)=\left(\sum_{\alpha(\kappa)\in\{\alpha(\kappa,z=L)\}}|\alpha(\kappa)|^2\right)-\frac{1}{2}. \tag{23}$$

We performed the procedure outlined above for interaction in 2-mm-long BBO crystal. The pump intensity was adjusted so that the total number of photons in the fluorescence field is near 10^8. This corresponds to the typical conditions found in noncollinear optical parametric amplifier- (OPA) (NOPA) used for amplification of ultrashort pulses [10].

For each of the various pump pulse durations, widths and crystal cut angles we performed ten independent simulations of classical fluorescence evolution. The average photon flux was computed according to the formula (23). Additionally, we assumed that $\bar{n}(\kappa)$ is almost independent of the angle around z axis and we averaged the results over this angle. This last step made ten independent simulations sufficient to calculate smooth intensity distributions.

Figure 8 shows the results of the simulations. The area of high intensity winds around the perfect phase-matching curve pictured in Fig. 3, as we argued before. In particular, for a given crystal cut angle θ the angle at which a particular frequency is emitted is nearly fixed. Note that the angular spread of the downconversion at a given frequency does not change with changing the pump beam waist. This is because the former is limited by the angular bandwidth of the phase matching in the crystal in our case. We find that the spectrum of the down-conversion is in general more sensitive to changing the pump beam waist from $w_p=80-160$ μm than it is to switching the length of the pumping pulses from $\tau_p=60-120$ fs. For a focused beam we observe more narrowband spectrum, except the crystal cut at $\theta=40°$ when we achieve broadband generation regardless of the pumping.

Qualitatively, the intensity along the perfect phase-matching curve changes as predicted by the perturbation theory and plotted in Fig. 6. This can be considered an unexpected success of the perturbation theory and may be qualitatively explained as follows. The process of parametric amplification with intense pumping leads to intense fluorescence fields, which exhibit mainly classical properties. In particular, $1/2$ in Eq. (23) can be neglected, which makes the process virtually identical to a classical amplification of a weak, white noise. In the course of interaction the components of the fluorescence become pairwise correlated. To some extent, the noiselike fluorescence can be separated into pairs of peaks which have approximately opposite k_x and k_y and frequencies summing up to the frequency of the pump, $2\omega_0$. Most of such pairs quickly diverge away from the pump pulse, but some propagate with it experiencing exponential growth. This is very similar to the mechanism behind the intensity of the fluorescence in a single pair generation regime, hence the intensity profiles are similar.

It is worthwhile to compare the numerical results from Fig. 8 with Figs. 4 and 5. We find that for short pump pulses the temporal walk-off between the pump and the fluorescence must be very small to achieve intense generation. For

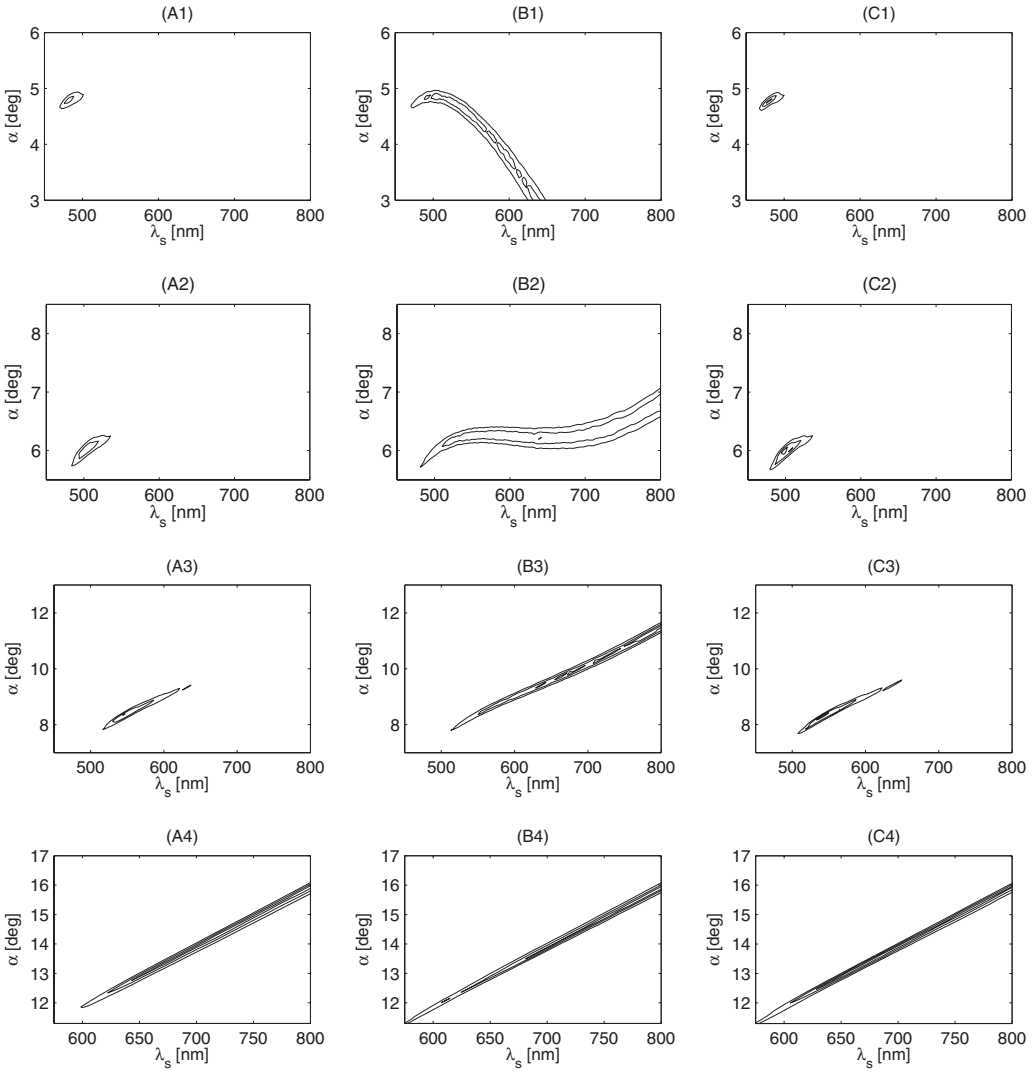

FIG. 8. The contour plot of the averaged photon flux of the fluorescence as a function of the angle $\alpha=\arcsin(c|k_x|/\omega)$ and the wavelength $\lambda=2\pi c/\omega$ for a 2-mm-long BBO. Each row corresponds to different crystal cuts: $\theta=29°$ (first row), $\theta=31.3°$ (second row), $\theta=35°$ (third row), and $\theta=40°$ (fourth row). Each column corresponds to different pump parameters: column A is for $\tau_p=60$ fs, $w_p=80$ μm; column B is for $\tau_p=60$ fs, $w_p=160$ μm; and column C is for $\tau_p=120$ fs, $w_p=80$ μm. The contour lines were drawn at 0.25, 0.5, and 0.75 of the maximum of each plot.

longer pulses, this requirement is relaxed and our calculations reveal broadband parametric generation.

V. CONCLUSIONS

In this paper we adopted perturbative and Wigner stochastic approaches to the task of calculating an intensity of the parametric fluorescence. In a single pair generation limit, original analytical expressions for the down-converted field can be derived. By linearizing the phase-matching function we found simple formulas for the intensity of the fluorescence in this regime. Photon flux of the signal depends on the temporal and spatial walk-off between the idler and the pump. In the case of type-I interaction in BBO this leads to peaks in the spectrum of the down-conversion signal at the frequencies where group velocity of the idler matches up with the pump.

Note that our derivations did not rely on any specific properties of type-I phase matching. Photon flux will depend on the group velocity mismatch and spatial walk-off also for other configurations of polarizations. Naturally, one must not forget that those quantities will change depending on the interaction type.

In an intense pumping case we performed a number of numerical stochastic simulations. We found that the calculated spectrum of the fluorescence exhibits the same features as predicted by the perturbative approximation. However, the contrast between the wavelengths at which the fluorescence is intense and those at which it is weak is more apparent due to exponential character of amplification in non-perturbative regime. In our view this is an important finding, since in many cases one may perform simple analytical calculations instead of tedious, three-dimensional stochastic simulations.

We conjecture that the group velocity mismatch and spatial walk-off are the crucial factors determining the bright-

ness of the down-conversion based photon sources. This is supported by similar brightness of two commonly used sources of entangled photon pairs: BBO type I in nearly collinear geometry [20] and noncolinear type-II source [1], which indeed exhibit similar group velocity differences.

Let us note that in practical situations the group velocity difference and walk-off can be varied by changing the orientation of the crystal, phase matching type and the crystal. One example is presented in the text above, where adjusting the crystal cut angle changed the wavelength of photons emitted from type-I BBO source.

Results presented in this paper facilitate comparison of various possible crystals, phase-matching types, and geometries at a source design stage. However, our findings apply to sources in which plane monochromatic waves are effectively observed. Geometries using single mode fiber coupling set to collect highly divergent spatial modes may require more complicated treatment [19].

The above results could be also used for optimization of parametric amplifiers, in which one seeks minimal contribution from the parametric fluorescence. From this point of view both group velocity difference $\Delta\beta_1'$ and spatial walk-off $\Delta\rho'$ should be made as high as possible. Unfortunately, increasing $\Delta\beta_1'$ reduces the spectral bandwidth, while increasing $\Delta\rho'$ reduces angular bandwidth of the amplifier. Therefore both group velocity difference $\Delta\beta_1'$ and spatial walk-off $\Delta\rho'$ should be set to values providing optimal tradeoff between parametric fluorescence intensity and the bandwidth of the amplifier. In practice changing $\Delta\beta_1'$ can be accomplished by tilting the crystal and changing the angle between the pump and signal beams. An important conclusion from our results is that the bandwidth should be made as narrow as possible in a given application. On the other hand, the ratio of the walk-off angle times crystal length to the pump beam diameter $L\Delta\rho'/w_p$ can be then independently adjusted by changing the pump beam waist w_p. In practice the w_p also controls the pump power density and the parametric gain. For very small w_p the length over which signal and pump beams overlap is reduced, thus reducing available gain. We conclude that w_p should be made as small as possible without damaging the crystal while at the same time the diameter of the seed beam sent to the amplifier should be increased along optic axis, so that amplification takes place in the entire crystal length.

ACKNOWLEDGMENTS

We acknowledge insightful discussions with Konrad Banaszek, Marek Trippenbach and Czesław Radzewicz, as well as financial support from a Polish Government scientific grant (2007-2009).

APPENDIX A

In this appendix we provide an explicit expression for $k^0(\omega)$ from Eq. (15). Note, that the set of Eqs. (14) yields

$$k_{pz}(2\omega_0,0,0) - k_z(\omega,k_x,k_y) - k_z(2\omega_0-\omega,-k_x,-k_y) = 0.$$

Using Eqs. (1) and (4) we obtain

$$\sqrt{k_x^2+k_y^2} = k^0(\omega) \equiv \frac{1}{2k_{pz}(2\omega_0)}\{4k_z^2(\omega)k_z^2(2\omega_0-\omega) - [k_{pz}^2(2\omega_0) - k_z^2(\omega) - k_z^2(2\omega_0-\omega)]^2\}^{1/2}.$$

This expresses $k^0(\omega)$ in terms of material and pump parameters as

$$k_{pz}(2\omega_0) = \frac{n_e(2\omega_0)n_o(2\omega_0)}{\sqrt{n_0^2(2\omega_0)\cos^2\theta + n_e^2(2\omega_0)\sin^2\theta}}\left(\frac{2\omega_0}{c}\right),$$

$$k_z(\omega) = n_o(\omega)\frac{\omega}{c}.$$

APPENDIX B

In this appendix we provide a detailed derivation of Eq. (16). Note that a surface of perfect phase matching is given by $\sqrt{k_x^2+k_y^2}=k^0(\omega_{\mathrm{obs}})$. Due to cylindric symmetry we can restrict the problem to $k_y=0$. We expect that largest contribution to the intensity of parametric fluorescence comes from κ and κ' such that $\Delta k_z(\kappa,\kappa')$ is small. Thus we linearize wave vector mismatch around $\kappa_0=(\omega_{\mathrm{obs}},k^0(\omega_{\mathrm{obs}}),0)$ and $\kappa_0'=(2\omega_0-\omega_{\mathrm{obs}},-k^0(\omega_{\mathrm{obs}}),0)$ with ω fixed. As a result, we obtain

$$\Delta k_z^{\mathrm{lin}}(\kappa,\kappa') = k_{pz}^{\mathrm{lin}}|_{\kappa_0+\kappa_0'} - k_z^{\mathrm{lin}}|_{\kappa_0} - k_z^{\mathrm{lin}}|_{\kappa_0'}.$$

Here,

$$k_{pz}^{\mathrm{lin}}|_{\kappa_0+\kappa_0'} = \left.\frac{\partial k_{pz}(\kappa_p)}{\partial\omega'}\right|_{\kappa_0+\kappa_0'}[\omega' - (2\omega_0-\omega_{\mathrm{obs}})] + \left.\frac{\partial k_{pz}(\kappa_p)}{\partial k_{px}}\right|_{\kappa_0+\kappa_0'}(k_x+k_x') + \left.\frac{\partial k_{pz}(\kappa_p)}{\partial k_{py}}\right|_{\kappa_0+\kappa_0'}(k_y+k_y'),$$

$$k_z^{\mathrm{lin}}|_{\kappa_0} = \left.\frac{\partial k_z(\kappa)}{\partial k_x}\right|_{\kappa_0}[k_x - k^0(\omega_{\mathrm{obs}})] + \left.\frac{\partial k_z(\kappa)}{\partial k_y}\right|_{\kappa_0}k_y,$$

$$k_z^{\mathrm{lin}}|_{\kappa_0'} = \left.\frac{\partial k_z(\kappa')}{\partial\omega'}\right|_{\kappa_0'}[\omega' - (2\omega_0-\omega_{\mathrm{obs}})] + \left.\frac{\partial k_z(\kappa')}{\partial k_x'}\right|_{\kappa_0}\times[k_x' + k^0(\omega_{\mathrm{obs}})] + \left.\frac{\partial k_z(\kappa)}{\partial k_y'}\right|_{\kappa_0}k_y'.$$

Using the definitions from Eq. (17) we obtain Eq. (16).

[1] P. G. Kwiat, K. Mattle, H. Weinfurter, A. Zeilinger, A. V. Sergienko, and Y. Shih, Phys. Rev. Lett. **75**, 4337 (1995).
[2] N. Gisin, G. Ribordy, W. Tittel, and H. Zbinden, Rev. Mod. Phys. **74**, 145 (1948).
[3] D. Bouwmeester, J.-W. Pan, K. Mattle, M. Eibl, H. Weinfurter, and A. Zeilinger, Nature (London) **390**, 575 (1997).
[4] W. P. Grice, A. B. U'Ren, and I. A. Walmsley, Phys. Rev. A **64**, 063815 (2001).
[5] V. Giovannetti, L. Maccone, J. H. Shapiro, and F. N. C. Wong, Phys. Rev. Lett. **88**, 183602 (2002).
[6] A. B. U'Ren, K. Banaszek, and I. A. Walmsley, Quantum Inf. Comput. **3**, 480 (2003).
[7] M. Tsang and D. Psaltis, Phys. Rev. A **71**, 043806 (2005).
[8] M. O. Scully and M. S. Zubairy, *Quantum Optics*, 1st ed. (Cambridge University Press, Cambridge, 1997).
[9] W. Wasilewski, A. I. Lvovsky, K. Banaszek, and C. Radzewicz, Phys. Rev. A **73**, 063819 (2006).
[10] T. Wilhelm, J. Piel, and E. Riedle, Opt. Lett. **22**, 1494 (1997).
[11] F. Tavella, A. Marcinkevicius, and F. Krausz, New J. Phys. **8**, 219 (2006).
[12] J. M. Vogels, K. Xu, and W. Ketterle, Phys. Rev. Lett. **89**, 020401 (2002).
[13] A. Perrin, H. Chang, V. Krachmalnicoff, M. Schellekens, D. Boiron, A. Aspect, and C. I. Westbrook, Phys. Rev. Lett. **99**, 150405 (2007).
[14] A. A. Norrie, R. J. Ballagh, and C. W. Gardiner, Phys. Rev. Lett. **94**, 040401 (2005).
[15] P. Deuar and P. D. Drummond, Phys. Rev. Lett. **98**, 120402 (2007).
[16] Y. B. Band and M. Trippenbach, Phys. Rev. Lett. **76**, 1457 (1996).
[17] M. I. Kolobov, Rev. Mod. Phys. **71**, 1539 (1999).
[18] Y. B. Band, C. Radzewicz, and J. S. Krasiński, Phys. Rev. A **49**, 517 (1994).
[19] A. Dragan, Phys. Rev. A **70**, 053814 (2004).
[20] P. G. Kwiat, E. Waks, A. G. White, I. Appelbaum, and P. H. Eberhard, Phys. Rev. A **60**, R773 (1999).